Array-Antenna Decoupling Surface

Ke-Li Wu, *Fellow, IEEE*, Changning Wei, Xide Mei, and Zhen-Yuan Zhang

***Abstract*— Massive multiple-input multiple-output (M-MIMO) technology is considered to be a key enabling technology for future wireless communication systems. One of the challenges in effectively implementing an advanced precoding scheme to a large-scale array antenna is how to reduce the mutual coupling among antenna elements. In this paper, a new concept that is called array-antenna decoupling surface (ADS) for reducing the mutual coupling between antenna elements in a large-scale array antenna is proposed for the first time. An ADS is a thin surface that is composed of a plurality of electrical small metal patches and is placed in front of the array antenna. The partially diffracted waves from the ADS can be controlled to cancel the unwanted coupled waves. Two practical design examples are given to illustrate the design process and considerations, and to demonstrate the usefulness of ADS for the applications of phased array antennas and M-MIMO systems when commonly used precoding schemes are applied. The attractive features of ADS include its applicability to a large-scale array antenna; suitability for a wide range of antenna forms; wide decoupling bandwidth; and simplicity in implementation.**

***Index Terms*— Decoupling, decoupling surface, large-scale array antenna, massive multiple-input multiple-output (M-MIMO), mutual coupling, phased array.**

I. Introduction

IT IS an indisputable fact that the massive multiple-input multiple-output (M-MIMO) system will be a key enabling technology in the future fifth-generation (5G) wireless communication systems. In an M-MIMO system, the number of antenna elements on a base station antenna is much larger than that of users served. To confront various emerging challenges facing this new technology for future commercial applications, intensive research on the practical implementation of the technology has been done from both theoretical and practical perspectives. It has been shown that an M-MIMO system can provide unprecedented high spectral efficiency and energy efficiency provided that the spatial correlation and mutual coupling among antenna elements are sufficiently weak [1], [2].

Due to limited space constrains for deploying a large number of antenna elements in an array, it is difficult to reduce mutual coupling effects by increasing the spacing between antenna elements. In fact, the mutual coupling effect in a large-scale array antenna has aroused a great deal of attention in the domains of phased array radars, wireless communications, and array signal processing since array antennas were put into use during the World War II [3]. Recently, people find that mutual coupling may seriously degrade the output signal-to-interference-noise ratio of an adaptive-array antenna and the convergence of array signal processing algorithms [4], [5]. An important early work that addresses the impact of mutual coupling effects on the performance of an MIMO system is [6], in which a significant drop of the mean capacity of an MIMO system due to the mutual coupling among antenna elements in a base station array antenna is demonstrated. Additionally, it is found that the mutual coupling in a transmitter array antenna not only affects the radiated power but also the power collection capability, implying that the channel transfer matrix depends on the active loading effect in an MIMO system [7]. To compensate mutual coupling and to design a compact large-scale MIMO system, much efforts have been paid to optimize precoding strategies on both the receiver and the transmitter sides [8], [9].

Although the mutual coupling effect embedded in the received signals of an adaptive array antenna system can be accommodated by increasing the complexity of algorithms for calculating the correlation coefficients, the impact of mutual coupling on the active reflection coefficient [10] of each antenna element can never be underestimated. A recent study shows that due to the mutual coupling effect in an MIMO array antenna, MIMO transmission is very stressful when a set of coded weighting coefficients are applied to the array antenna because of random like phase shifts on antenna elements; showing that the worst voltage standing wave ratio (VSWR) can be as high as 6 for the mutual coupling level of −15 dB or more than 2 for the level of −20 dB [11]. A caution is given when designing an MIMO transmission system; the mutual coupling effect must be alleviated to avoid high VSWR at transmitter ports.

An array antenna containing a large number of elements is prone to suffer from a certain degree of mutual coupling among antenna elements. It is particularly true for a compact array antenna such as the MIMO array antennas for 5G wireless communication systems and compact phased array antennas for advanced radars. For more than half a century, the struggle to reduce mutual coupling has never been stopped. A well-recognized pioneer work toward this direction was proposed in 1976 [12], in which a transmission line network is introduced between every pair of antenna elements. The network, whose mutual admittance is opposite to that of the coupled antenna elements, cancels the mutual

Manuscript received October 28, 2016; revised April 26, 2017; accepted May 27, 2017. Date of publication June 7, 2017; date of current version November 30, 2017. This work was supported by Postgraduate Scholarship of The Chinese University of Hong Kong. *(Corresponding author: Ke-Li Wu.)*

The authors are with the Department of Electronic Engineering, The Chinese University of Hong Kong, Hong Kong (e-mail: klwu@ee.cuhk.edu.hk; cnwei@ee.cuhk.edu.hk; xdmei@ee.cuhk.edu.hk; zyzhang@ee.cuhk.edu.hk).

Color versions of one or more of the figures in this paper are available online at http://ieeexplore.ieee.org.

Digital Object Identifier 10.1109/TAP.2017.2712818

coupling between the antenna pair in the narrowband sense. This concept has been further developed by many different variations. Until very recently it is found that by replacing the transmission line network by a coupled resonator network a wide band decoupling and matching can be achieved for two coupled low gain antennas [13], [14]. Obviously, such decoupling approaches are only effective for two coupled antennas as any additional shunt connection of a decoupling network will affect the performance of the existing decoupled antennas.

Unlike all the existing decoupling methods for two antennas, decoupling of multiple antenna elements in an array antenna is much more challenging. Although a number of literatures in this area are available, to save space, only those representative works are reviewed here. In [15], the mutual coupling owing to surface waves of a thick substrate is utilized to form an interference signal to cancel the directly coupled signal between two microstrip antennas, creating a deep null in the mutual coupling. Because the decoupling performance of this approach is restricted by the properties of the thick substrate and the separation distance of the two antennas, as admitted in the paper, the application of the approach to an array antenna is likely to be an issue. Nevertheless, the attempt to conquer the mutual coupling effect continues. An electromagnetic band-gap (EBG) structure is inserted between two microstrip antennas, resulting in lowering the mutual coupling level [16].

To the best understanding of the authors, basically, the role of the EBG structure inserted is to adjust the magnitude and phase of the surface wave to create an appropriate interference to the coupled waves. This explanation can be justified by the observed deep notch in the isolation parameter when substrate parameters are chosen appropriately to support a right amount of surface waves. The separation distance and dimensions the EBG structure also need to be appropriate to support the opposite phase of the coupled waves. To satisfy the magnitude and phase conditions simultaneously is not a trivial job in a practical design as there is no space to host an effective artificial structure between antenna elements.

Dummy elements can sometimes be used to generate required interferences against mutual coupling among coupled antenna elements by multiple reflections. A network representation for determining the optimal reactive loads of dummy elements is proposed [17]. The main limitation of such decoupling approaches is that it requires enough spaces to “plant” sufficient number of dummy elements followed by good wishes. Obviously, the approach is not suitable for planar array antennas for M-MIMO base stations, where a large number of high-gain antenna elements will be employed. Needless to say, a systematic way is required to decouple an array antenna involving a large number of co- and cross-polarized antenna elements.

Although the mutual coupling problem in a large-scale array antenna for various applications is disturbing and is urgent to solve for future wireless communication systems, to the best knowledge of the authors, so far there is no such a systematic and effective approach to reduce mutual coupling among antenna elements, both in co- and cross-polarizations, in an array antenna with a large number of elements. To confront the problem, a new decoupling approach dedicated for broadside radiation array antennas, which is named as array-antenna decoupling surface (ADS), is proposed and experimentally demonstrated in this paper. An ADS is a thin surface that is composed of a plurality of electrical small metal reflection patches and is placed less than one-half the wavelength above the ground plane of an array antenna. An ADS is ingeniously designed to create partial reflective electromagnetic (EM) waves to cancel the coupled waves from the adjacent antenna elements. By appropriately adjusting the distance between the ADS and the array antenna and the sizes of the patches, the out of phase and the equal intensity conditions of the interference waves relative to that of the unwanted coupled waves can be achieved, leading to a high degree of cancellation of the unwanted mutual coupling between adjacent antenna elements.

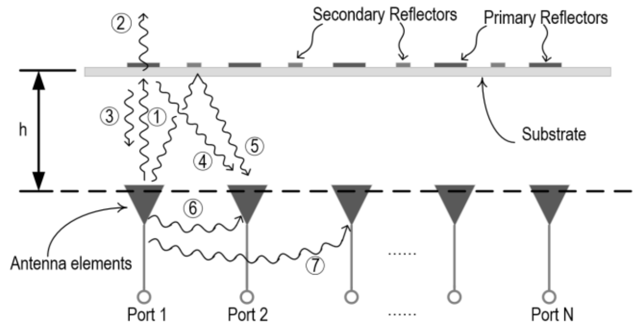

Fig. 1. Schematic of an array antenna and an ADS with spacing distance h.

The following unique and attractive features of the proposed ADS method will be demonstrated:

1) applicability to a large-scale array with a wide range of antenna forms of both single and dual-linear polarizations;
2) preservability of radiation characteristics and matching conditions of original antenna elements;
3) superiority of wide band decoupling;
4) simplicity in implementation.

This paper consists of five sections. Section II describes the basic concept of ADS. Practical design considerations of ADS are illustrated through the design process of an ADS for a simple 1 by 8 linear air patch array antenna in Section III. The design of an ADS for a practical 2 by 2 dual-polarized array antenna consisting of eight planar dipole elements is also discussed in great details in Section IV, demonstrating the effectiveness and usefulness of the ADS method in applications for radars and M-MIMO systems. Conclusion is given in Section V.

II. Concept of ADS

The schematic of an array antenna with a generic ADS is shown in Fig. 1. An ADS is a thin layer of low-loss and low dielectric constant substrate printed with a plurality of electrical small metal reflection patches. The geometries and the dimensions of the patches are carefully designed to create a right amount of diffracted waves at the port of the coupled antenna element to cancel the coupled waves while minimizing the perturbation to the original array antenna. The separation distance (h) between the ADS and the ground plane of the array antenna is determined to ensure that the partial diffracted wave is out of phase of the coupled waves at the port of the coupled antenna element.

As depicted in Fig. 1, it can be perceived that for an array antenna with an ADS the energy radiated from an element ① consists of four portions: the wave being radiated outward into far space ②; the reflected wave received by the transmitting antenna ③; the reflected wave from the primary reflector patches ④; and the reflected wave from the secondary reflector patches ⑤. The primary objective of using ADS is to reduce the mutual coupling between two adjacent antenna elements ⑥ while not deteriorating the mutual coupling among nonadjacent antenna elements ⑦, which are assumed to be weak enough to worry about. As an ADS is located in the reactive region of an array antenna, use of the word "reflected wave" is never accurate. It is used only to mean the diffracted waves of an ADS that are received by antenna elements.

As illustrated in Fig. 1, an ADS provides a second signal path between the coupled and the coupling antenna elements. Since the second signal can be controlled to be with the same intensity and the opposite phase as that of the aggregated coupled signal (the first signal) by carefully designing the pattern and the dimensions of reflection metal patches on the ADS and the distance h, coupling between adjacent antenna elements can be significantly canceled by the reflected waves from the ADS. In terms of functionality, the reflection patches can be classified in two types: the primary reflectors and the secondary reflectors. The primary reflectors are designed to provide major reflected waves, usually in the same polarization as that of the coupled waves, and the secondary reflectors are designed to create minor reflected waves to mitigate weaker mutual coupling such as the mutual coupling in cross-polarization, or to fine tune the major reflected waves.

ADS can be easily applied to a 2-D array antenna. ADS can be printed on a thin layer of low-loss substrate. A nonplanar conformal ADS is also feasible but with more design efforts. Therefore, to integrate an ADS with an antenna radome could be an attractive option.

III. Design Considerations of ADS

Designing an ADS is not only a subject of science but also a creation of an art work. Conceiving a legitimate pattern of the metal reflection patches on an ADS requires a very good understanding of the field distribution in the vicinity of the coupling and coupled antenna elements and intuition of how to control the reflected waves. ADS can take multiple design options for a given array antenna. Fig. 2 shows some of possible geometries of the metal reflection patches: 1) for linearly polarized antenna elements [Fig. 2(a)]; 2) for dual-polarized antennas elements [Fig. 2(b)]; 3) for circularly polarized antennas [Fig. 2(c)]; and 4) for some of composite configurations that may provide more design flexibilities in both magnitude and phase controls [Fig. 2(d)]. Among all the possible geometries, the rectangular and the cross-shaped patches are simplest and most effective for both the single and dual-linearly polarized array antennas. In order to minimize

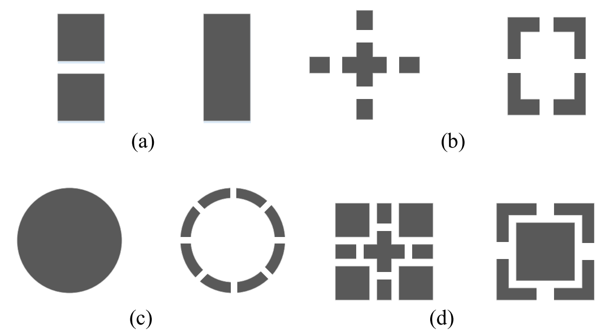

Fig. 2. Some geometries of metal reflection patches. (a) Patches for linearly polarized antennas. (b) Patches for dual-polarized antennas. (c) Patches for circularly polarized antennas. (d) Some composite patches.

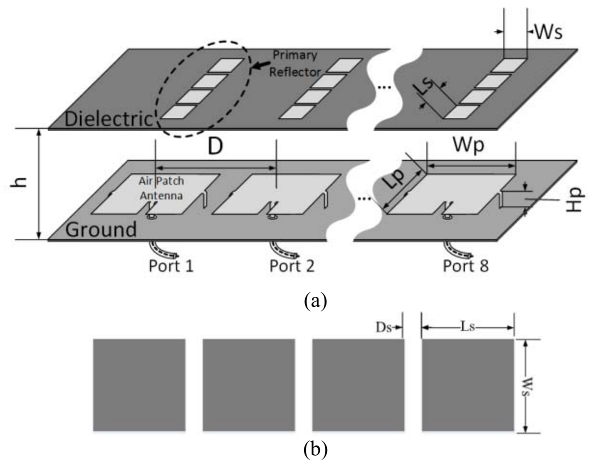

Fig. 3. (a) Eight-element linearly polarized air patch array antenna and an ADS with eight metal broken strips. (b) Dimensions of a metal broken strip.

the perturbation to the original array antenna, a broken patch consisting of a number of small metal patches instead of a large patch is preferred to avoid any resonance effect. As a guideline, the largest dimension of a patch is less than one-third of the wavelength. Usually, ADS consists of a group of primary reflector patches to create the main reflected waves and a few of secondary reflector patches to compensate the missing components of the main reflected waves.

In addition to geometrical dimensions, the separation distance h is also a key design parameter. To be easy to follow, the eight-element linear air patch array antenna shown in Fig. 3, which will be fully discussed in Section III, is used as a "hello world" example to illustrate the design process. This array antenna operates in the 2.45-GHz Industrial, Scientific, and Medical (ISM) band. Since the major field component of every two adjacent elements are the same, as shown in Fig. 3(a), eight primary rectangular reflectors, each of which is broken into four pieces of small patches, are printed on the ADS substrate. In fact, a rectangular reflector strip can also be broken into other number of pieces as long as resonant frequency of the reflector strip is not close to the working frequency of the array antenna. Fig. 3(b) depicts the details of the broken reflector strip. The dimensions of the antenna element and the ADS are given in Table I. Because the gap D_s is not very sensitive to the decoupling performance, it is set to 1 mm. In this example, each rectangular reflector strip is placed right

TABLE I
DIMENSIONS OF THE EIGHT-ELEMENT AIR PATCH ARRAY IN mm

Wp	*Lp*	*Ls*	*Ws*	*Hp*	*Ds*	*h*	*D*
45	52.5	15	15	7	1	38	55

above its corresponding antenna element and is in-line with the polarization direction. Nevertheless, other arrangements are also possible. Using broken metal rectangular reflectors instead of a long strip is to avoid creating resonance near the working frequency by the ADS while still introducing sufficient amount of reflections. A well-designed ADS will minimize the reflected wave ③ shown in Fig. 1, and not change the matching condition of each antenna element significantly.

The decoupling conditions of the ADS can be easily explained using S-parameters of two coupled antennas with and without applying an ADS. Taking the mutual coupling between elements 1 and 2 as an example and assuming that the matching conditions of the two elements with and without ADS are sufficiently good. With an ADS, the reflected wave that is transmitted from element 1 and received by element 2 can be expressed by

$$S_{21}^{\text{Refl}} = S_{21}^{\text{ADS}} - S_{21}^{\text{Array}} \tag{1}$$

where S_{21}^{ADS} is the S_{21} parameter measured at the two antenna ports when the ADS is applied, and S_{21}^{Array} is the S_{21} parameter of the original array antenna without the ADS. Therefore, the decoupling conditions of the two antenna ports, or the condition for $S_{21}^{\text{ADS}} = 0$ are

$$|S_{21}^{\text{Refl}}| = |S_{21}^{\text{Array}}| \tag{2a}$$

$$\text{Phase of } (S_{21}^{\text{Refl}}) = \text{Phase of}(S_{21}^{Array}) + \pi. \tag{2b}$$

Intuitively, the height of the ADS above the antennas determines the phase of the partial reflected wave and the size of the reflection metal reflector on the ADS controls the intensity of the partial reflected wave. This intuition can be well justified by a parametric study. Fig. 4(a) shows the magnitude difference of $|S_{21}^{\text{Refl}}| - |S_{21}^{\text{Array}}|$ verses frequency for different heights h, from 29 to 44 mm. It is seen that the decoupling condition for magnitude at the center frequency of 2.45 GHz does not change very much. However, as shown in Fig. 4(b), the decoupling condition for the phase difference, which is calculated by the difference of the left-hand side (LHS) and the right-hand side (RHS) of (2b), varies in a range of 50°. With an appropriate set of dimensions of the ADS, as shown in Fig. 4(c), a wide range of heights can achieve a reasonable good decoupling level. The deepest decoupling level of the ADS can be achieved when the decoupling conditions for both the magnitude and the phase differences are satisfied at the center frequency of 2.45 GHz.

Fig. 5 shows how the sizes of the reflection patches affect the decoupling conditions and consequently the decoupling level. Fig. 5(a) states that as the size W_s of the reflection patches varies from 11 to 19 mm, the magnitude difference of $|S_{21}^{\text{Refl}}| - |S_{21}^{\text{Array}}|$ varies significantly. When the size varies

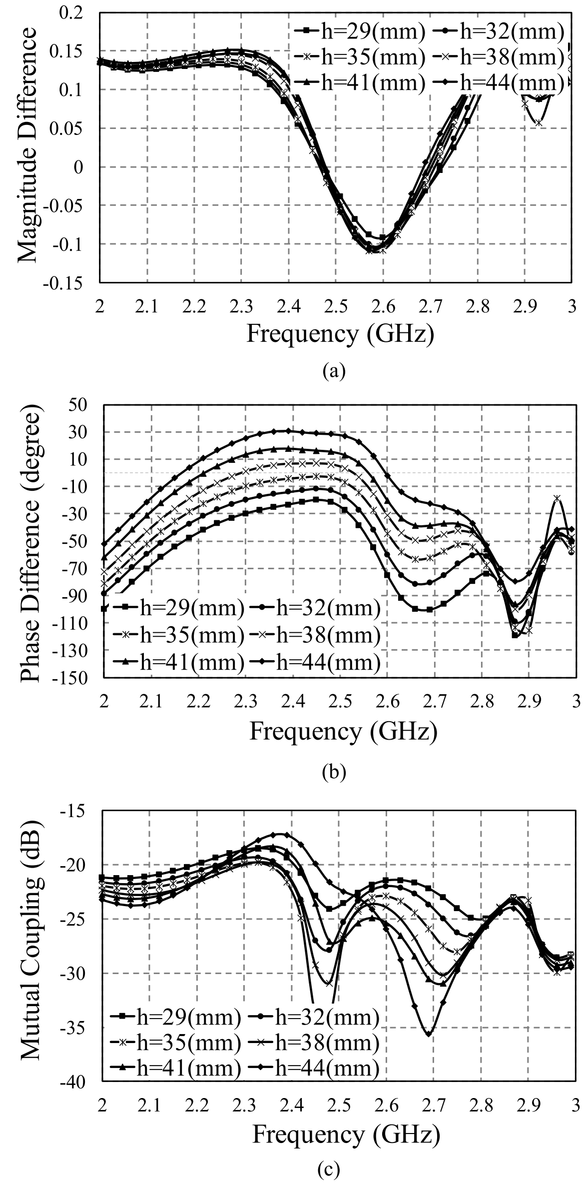

Fig. 4. Simulated (a) magnitude difference, (b) phase difference, and (c) mutual coupling with different heights and $W_s = 15$ mm and $D_s = 1$ mm.

between 15 and 17 mm, the decoupling condition for magnitude can be well satisfied at the center frequency. However, when the size becomes larger, the reflected wave tends to be stronger and the decoupling condition moves toward a lower frequency or conversely when the size is smaller. Fig. 5(b) shows the phase difference of the LHS and the RHS of (2b) for different sizes of W_s. When the size varies between 13 and 15 mm, the phase difference is close to zero in a wide frequency range. Two attractive properties of the ADS in satisfying the phase condition can be observed in Fig. 5(b): 1) the phase difference is insensitive to the variation of the size of the reflector and 2) the ripple of the phase difference is very small over a wide frequency range. Fig. 5(c) shows the overall decoupling level for different sizes of W_s when the height h is set to 38 mm. A deep notch at the center frequency is seen when the size W_s is close to 15 mm, indicating

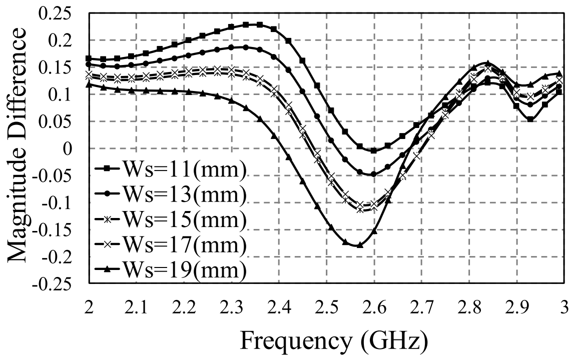

(a)

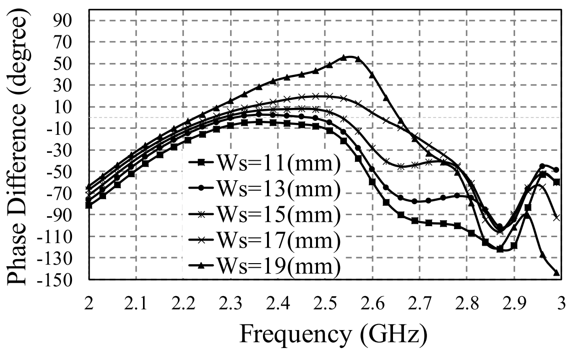

(b)

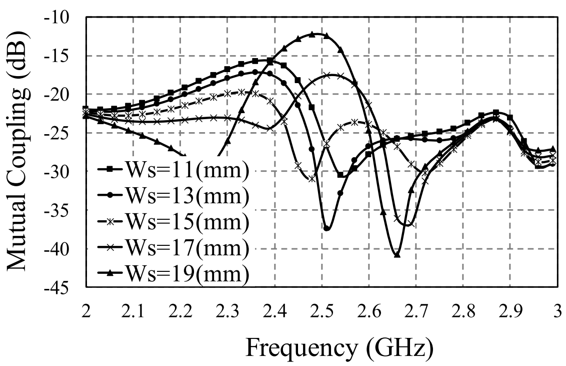

(c)

Fig. 5. Simulated (a) magnitude difference, (b) phase difference, and (c) mutual coupling with different sizes of metal strip and $h = 38$ mm.

that the reflected waves well interfere the unwanted mutual coupling.

In conclusion, the size of the reflection patches on the ADS decides the magnitude condition and the height of the ADS determines the phase condition. When the two conditions are well satisfied simultaneously, the deepest decoupling level can be achieved. Furthermore, when the two decoupling conditions are approximately satisfied, there is still a satisfactory decoupling improvement obtained in a wide frequency range.

IV. Design Examples

To demonstrate the ADS method for practical array antennas and to justify the importance of decoupling for an array antenna, two case studies will be conducted in this section. The first example is the eight-element linearly polarized air patch array antenna. The second example is a 2 by 2 dual-polarized array antennas working in a 5G frequency band. In both cases, the array antennas are EM designed using ANSIS HFSS, fabricated and fully measured. The usefulness of the ADS method is justified through the assessments of active reflection coefficients of antenna elements with a realistic precoding for 5G applications or weightings for a phased array application as well as element active radiation patterns.

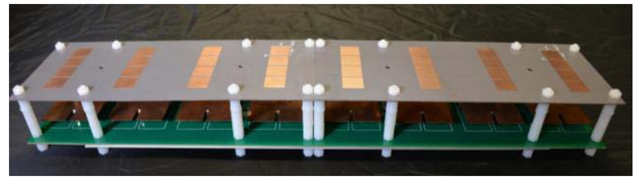

(a)

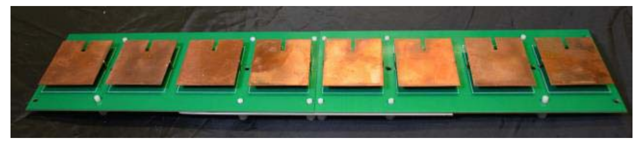

(b)

Fig. 6. Photograph of the prototype of (a) eight-element linear air patch array with the ADS and (b) array without the ADS.

A. Eight-Element Linear Air Patch Array Antenna

As shown in Fig. 3(a), each air patch antenna element working at 2.45 GHz is supported by three metal legs, two are located at the virtual short circuit points on the two nonradiating edges and one acts as the inset-feeding probe. The center-to-center spacing D of array elements is 55 mm or $0.45\lambda_0$. Following the design guidelines discussed in Section III, an ADS for the array is designed and prototyped. Photograph of the prototyped array antenna with and without the ADS is shown in Fig. 6(a) and (b), respectively. The substrate used for the ADS is with dielectric constant of 2.6, loss tangent of 0.001, and thickness of 1 mm. The other dimensions of the array antenna are listed in Table I.

The prototyped array antenna with and without the ADS are fully tested. The radiation characteristics are measured using the in-house SATIMO SG128 spherical near-field scanner in an ISO17025 accredited laboratory in the university. In measuring the concerned radiation patterns and S-parameters, other unmeasured antenna ports are terminated by 50-Ω loads. Fig. 7 shows the measured S-parameters at some of the interested antenna ports. Due to the symmetry of the array, only the S-parameters of port 1 through port 4 are presented. It is clearly seen that the mutual coupling between any two adjacent elements, say S_{12}, S_{23}, or S_{34}, is significantly reduced from about -15 dB to below -30 dB whereas the mutual coupling between nonadjacent elements, say S_{13}, maintains at the same level or is improved a little. It is worth mentioning that all the antenna ports are not rematched after applying the ADS, demonstrating that the ADS does not affect the matching condition of the original array antenna significantly. It is also seen that the decoupling bandwidth for mutual coupling being reduced from -15 dB to better than -24 dB is much wider than that of 10-dB return loss (RL), demonstrating the potential for a wide band decoupling. The radiation patterns of antenna elements 1 and 3 with and without the ADS are

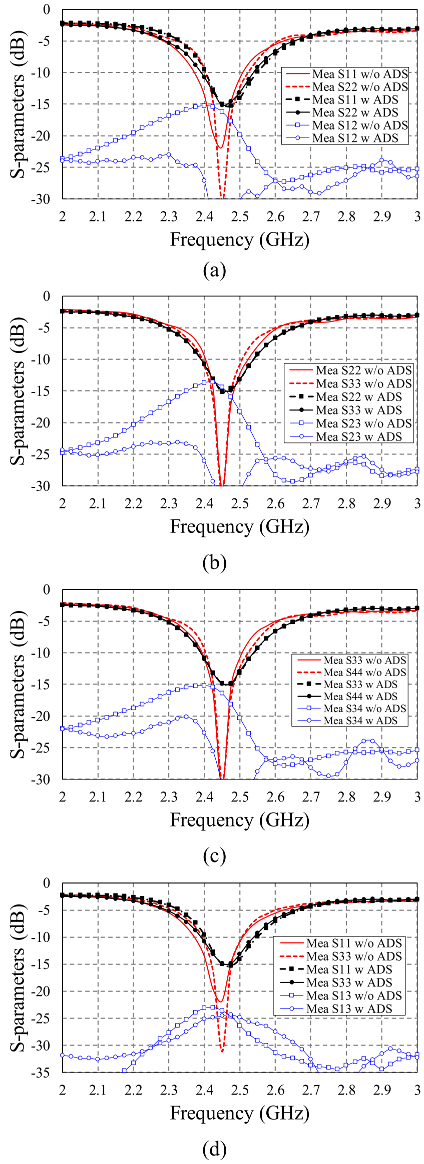

Fig. 7. Representative measured S-parameters of the eight-element air patch array with and without the ADS of (a) antennas 1 and 2, (b) antennas 2 and 3, (c) antennas 3 and 4, and (d) antennas 1 and 3.

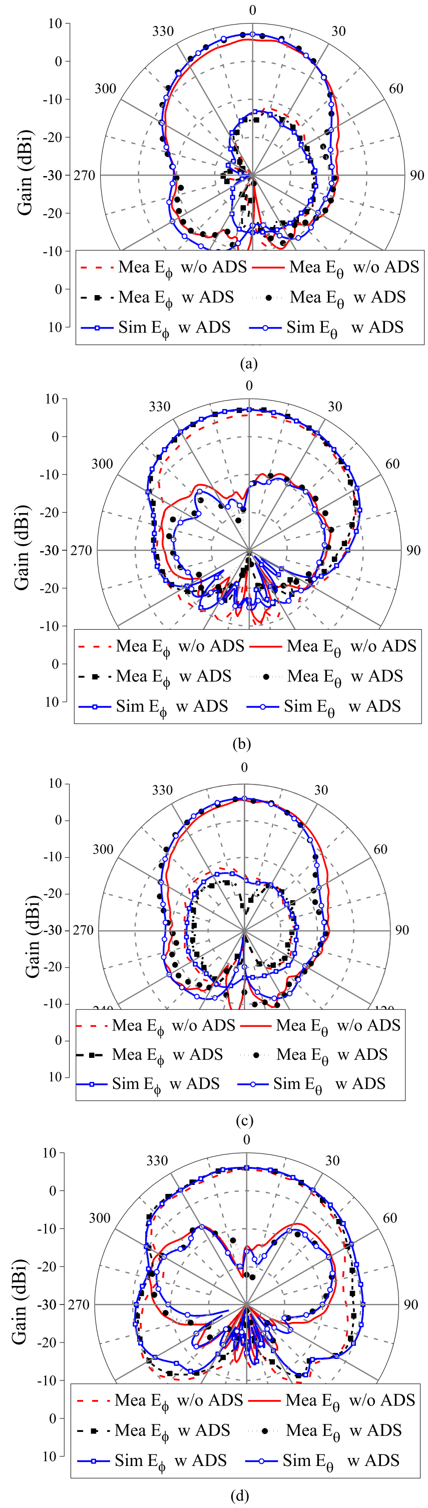

Fig. 8. Representative radiation patterns of the eight-element air patch array with and without the ADS. (a) E-plane patterns of element 1. (b) H-plane patterns of element 1. (c) E-plane patterns of element 3. (d) H-plane patterns of element 3.

presented in Fig. 8. It can be observed that for an edge antenna element, i.e., element 1, the antenna gain is apparently enhanced after applying the ADS. However, for an internal element, e.g., element 3, the gain improvement is not obvious. Nevertheless, the beam widths, both in the E- and H-planes, of the array elements with and without the ADS appear to be about the same. The measured radiation patterns for array elements with the ADS are verified by HFSS EM simulation. The correlation between the measured and the simulated is very good.

In this example, eight identical rectangular reflector strips are placed right above the eight identical elements one by one. Such arrangement is seemingly independent of the number of antenna elements. This attractive feature justifies the applicability of the ADS method to a large-scale array antenna.

In a 5G system, a base station antenna sends data streams to multiple users at the same time and in the same frequency band by applying a precoding scheme to the data stream to be transmitted at each antenna port of the array antenna. Several precoding schemes are discussed in [18], among which the zero-forcing (ZF) scheme is a popular one due to its simplicity. To demonstrate the practical importance of the

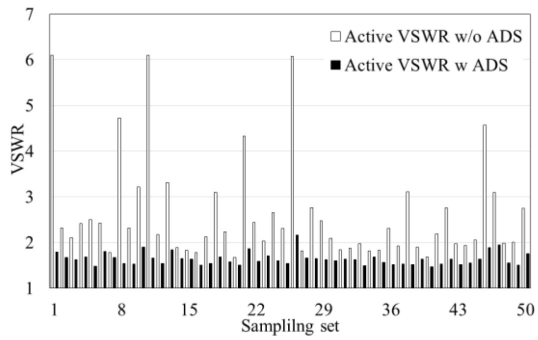

Fig. 9. Worst active reflection coefficients among the antenna ports of the eight-element array in frequency band of 50 MHz in 50 random sets of ZF precoding weighting coefficients.

ADS to an M-MIMO system, the active reflection coefficients of antenna elements in the array to which the weighting coefficients obtained by the ZF precoding scheme are applied, are investigated. The definition of active reflection coefficients can be found in a classical reference [10].

The ZF precoding is a beamforming scheme for generating weighting coefficients on an array antenna based on the estimated channel matrix. It intends to send data streams toward the corresponding multiple intentional users with nulls in the "directions" of other interfering users. It is reasonable to choose an uncorrelated Rayleigh fading channel model for demonstration purpose since spatial correlation between anonymous users can be neglected for a large-scale array antenna. The ZF weighting coefficients can be obtained by [19]

$$W_{\mathrm{ZF}} = H^{\dagger}(HH^{\dagger})^{-1} \quad (3)$$

where H is the transmission channel matrix with dimension of M by N, M is the number of users, and N is the number of antenna elements. It is assumed that four users are served by the eight-element linear array. To evaluate the system performance of an array antenna with and without the ADS, for simplicity, four random binary data streams are modulated by BPSK scheme to the carrier and are transmitted in a Rayleigh fading channel. Fifty sets of weighting coefficients are randomly generated by the ZF precoding scheme under the Rayleigh fading channel model. The acceptance magnitude threshold of the weighting coefficients is set to 0.1 to avoid extremely large active reflection coefficients. The largest active reflection coefficient among the eight antenna elements in the frequency band of 50 MHz is collected for each set of weighting coefficients and is shown in Fig. 9. It can be seen that by applying the ADS to the array antenna, the maximum active VSWR is significantly reduced for almost all the random sets of weighting coefficients.

To demonstrate the usefulness of the ADS for radar applications, in which the radiation pattern forms dedicated beams in multiple specific directions. The array factor (AF) can be expressed by the discrete Fourier transformation (DFT)

$$\mathrm{AF} = \sum_{m=0}^{M-1} I[m]e^{-jkmd\cos\theta} \quad (4)$$

TABLE II
DIMENSIONS OF THE 2 BY 2 DIPOLE ARRAY IN mm

La	*ha*	*Wa*	*D1*	*D2*	*Lg*	*Wg*	*H*
36.5	12.5	2	45	60	180	165	25

where $I[m]$ is the weighting coefficient on the mth antenna element, θ is the propagation direction, and d is the spacing between antenna elements. For given target beams in angular spectrum, the weighting coefficients can be obtained by applying inverse DFT. For example, two desired beams in the directions of 320° and 20° are targeted using the eight-element array antenna. The obtained weighting coefficients are shown in Fig. 10(a). The ideal synthesized AF and the simulated active radiation patterns with and without the ADS are superimposed in Fig. 10(b). The simulated active radiation patterns are obtained by applying the weighting coefficients to the port excitations in the HFSS models of the array with and without the ADS. It can be seen from Fig. 10(b) that the beam directions of the active radiation pattern without the ADS deviate from the synthesized due to the mutual coupling. The mutual coupling effect can be alleviated by applying the ADS. The active VSWR at each antenna port of an array antenna is another major concern in phased array antennas. Fig. 10(c) shows the largest active VSWR of each antenna element of the eight-element linear array in the frequency band with and without the ADS. It is seen that the ADS reduces the worst VSWR from 1.9 to less than 1.26, a very significant improvement.

B. 2 by 2 Dual-Polarized Eight-Element Linear Dipole Array

The second example is a 2-D dual-polarized 2 by 2 planar dipole array with eight elements operating in the frequency band from 3.3 to 3.8 GHz, one of the 5G frequency bands. The array antenna together with an ADS is illustrated in Fig. 11(a). This small-scale array antenna is a good reflection of a large-scale M-MIMO array antenna as the ADS decoupling solution can be easily scaled up to an M-MIMO array antenna with a large number of antenna elements of the same type.

In the 2 by 2 array, each antenna unit consists of two perpendicularly polarized dipole antennas, one is oriented in 45° and the other in 135°, with respect to the horizontal line. The two diamond ring-shaped arms of each dipole antenna with the width of W_a are printed on a substrate. The substrate is with dielectric constant of 2.6, loss tangent of 0.001, and thickness of 1 mm. Each dipole is fed by a microstrip line balun, which is installed vertically to each planar dipole [20]. As illustrated in Fig. 11(b), the horizontal and vertical center-to-center distances between two antenna units are $D1$ and $D2$, which are 45 and 60 mm, respectively. As shown in Fig. 11(c), the two perpendicular balun circuits also play the role of mechanical supporter to the two dual-polarized antennas. The ports of antenna elements are located on the other side of the ground plane. The assignment of element number is given in Fig. 11(d). The other major dimensions of the array are listed in Table II.

Designing a viable ADS requires a good understanding of the antenna working mechanism and a sense of art. Seeking

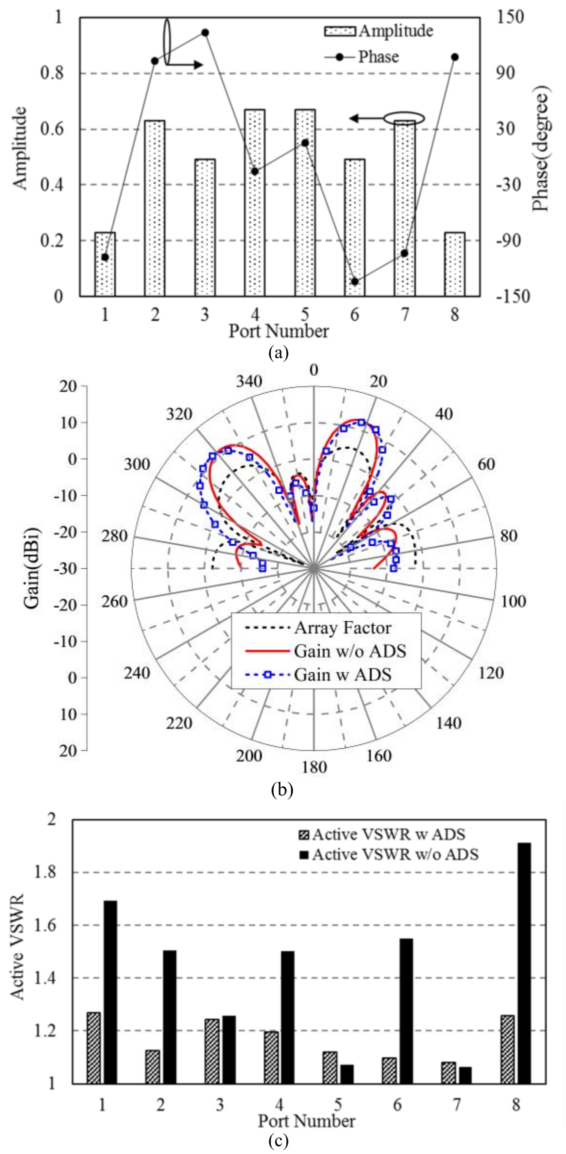

Fig. 10. (a) Weighting coefficients of the eight-element phased array. (b) Synthesized AF and the active radiation patterns of the array with and without the ADS. (c) Largest active VSWR at each antenna port with and without the ADS when the weighting coefficients are applied to the array.

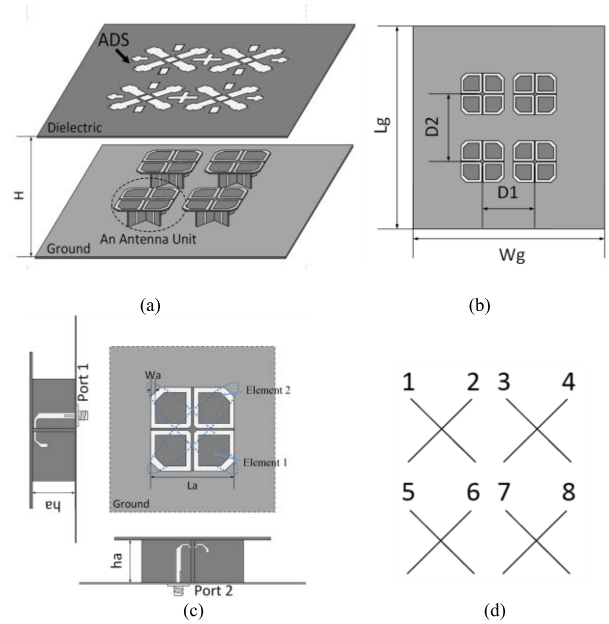

Fig. 11. 2 by 2 dual-polarized dipole array. (a) Perspective view of the array with the ADS. (b) Top view of the array. (c) Top and side views of one antenna unit consisting of two dual-polarized antenna elements. (d) Number assignment of the eight antenna elements.

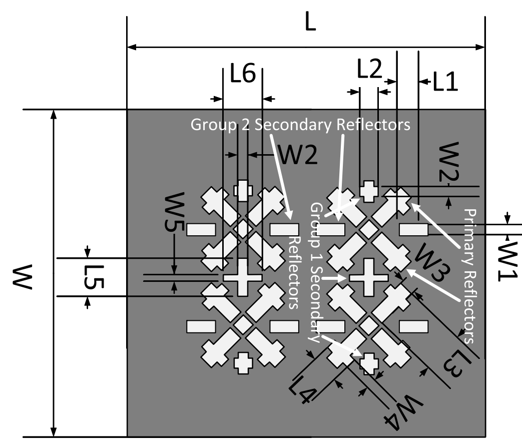

Fig. 12. Metal reflection patches on the ADS for the 2 by 2 dipole array.

the symmetry and maintaining the balance are two important components in art. Fig. 12 shows the metal reflection patches printed on the ADS substrate for the 2 by 2 array. The substrate used for the ADS is the same as that for the printed dipoles and the balun circuits. The ADS consists of eight primary reflectors and two groups of secondary reflectors. Each of the primary reflectors is oriented in-line with the corresponding dipole underneath symmetrically and is made of a broken metal strip. Two crossed primary reflectors for the two dual-polarized dipoles in an antenna unit are used to maintain the symmetry of the antenna unit. The main consideration to adopt a broken patch reflector for a primary reflector is to minimize the perturbation to the radiation patterns and the deterioration of the matching condition of the corresponding dipole antenna. A primary reflector is designed to cancel the strongest mutual co-polarized coupling between two adjacent elements in this 2-D array. Since $D2 > D1$ in this example, the mutual coupling between two horizontally adjacent elements, say elements 1 and 3, will be stronger than that of two vertically adjacent elements. Two groups of secondary reflector patches are used in the ADS design. The patches in group 1 are introduced to create a small amount of reflected wave in the cross-polarized components to cancel the mutual coupling between two cross-polarized adjacent elements, such as the coupling between elements 1 and 4 and that between elements 2 and 3. They are called secondary reflector patches because the reflected waves are at a much smaller level than those by the primary reflector patches. The secondary reflector patches play a role of “fine tuning” and their sizes are smaller than that of the primary reflector patches in general. Group 2 secondary reflector patches are introduced to adjust the reflected waves from the primary

TABLE III
DIMENSIONS OF ADS FOR THE 2 BY 2 DIPOLE ARRAY IN mm

L	*L1*	*L2*	*L3*	*L4*	*L5*	*L6*
170	9.5	8.5	20	14	18.5	18
W	***W1***	***W2***	***W3***	***W4***	***W5***	
155	5	5	7	8	3	

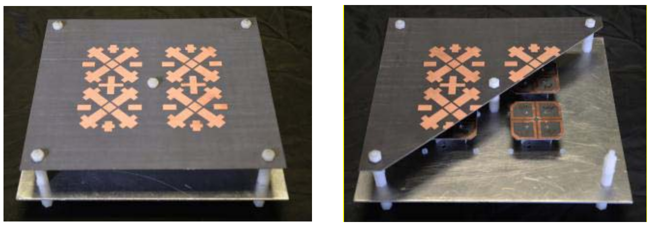

(a) (b)

Fig. 13. Photograph of the prototype of the 2 by 2 dipole array antenna with the ADS. (a) Array with the ADS on top. (b) Array with the ADS half cutoff.

reflector patches above two vertically adjacent antenna elements of co-polarization. This is needed because the mutual coupling between elements 1 and 3 is different from that between elements 1 and 5. Of course, to maintain the balance between two cross-polarized dipoles in the same antenna unit, some auxiliary patches of the secondary reflectors are added symmetrically about the antenna unit. Fig. 13(a) is a photograph of the prototyped 2 by 2 dipole array antenna with the designed ADS. For a clear view, a photograph of the array with a cutoff of the ADS is presented in Fig. 13(b). The detailed dimensions of the ADS are given in Table III.

Due to the symmetry of the 2 by 2 array, only the measured S-parameters of the concerned ports are presented in Fig. 14. As shown in Fig. 14(a), the RLs at port 1 and port 2 of the array with the ADS remain at 15 dB or better across the whole working frequency band from 3.3 to 3.8 GHz. The mutual coupling between two adjacent elements of the same polarization in both horizontal and vertical directions, i.e., S_{13} and S_{15}, is shown in Fig. 14(b). It is clearly seen that with the ADS, S_{13} is reduced from about −14 to −25 dB or lower, and S_{15} is improved from −26 to −28 dB or lower. As shown in Fig. 14(c), the coupling between two cross-polarized elements in the same unit, say S_{12}, is also improved to below −30 dB although the original coupling without the ADS is about −25 dB. The coupling between two adjacent dipoles with cross-polarization, say S_{14}, is difficult to control when the two antenna units are close to each other. This is because the coupling is strongly determined by the capacitance between the two closest ends of the concerned dipoles. However, it is seen from Fig. 14(c) and (d) that by introducing group 1 secondary reflectors, both S_{14} and S_{23} are reduced from −23 to −25 dB and from −25 to −30 dB or lower, respectively. Usually, the mutual coupling between two co-axial and colinear dipoles, say S_{17}, and that between two far away dipoles of co-polarization, say S_{28}, are inherently low before applying the ADS. There are no specific considerations to deal with the mutual coupling rather than not deteriorating it. As can be observed in Fig. 14(d) that with the major mutual coupling reduced the weak mutual coupling is also reduced.

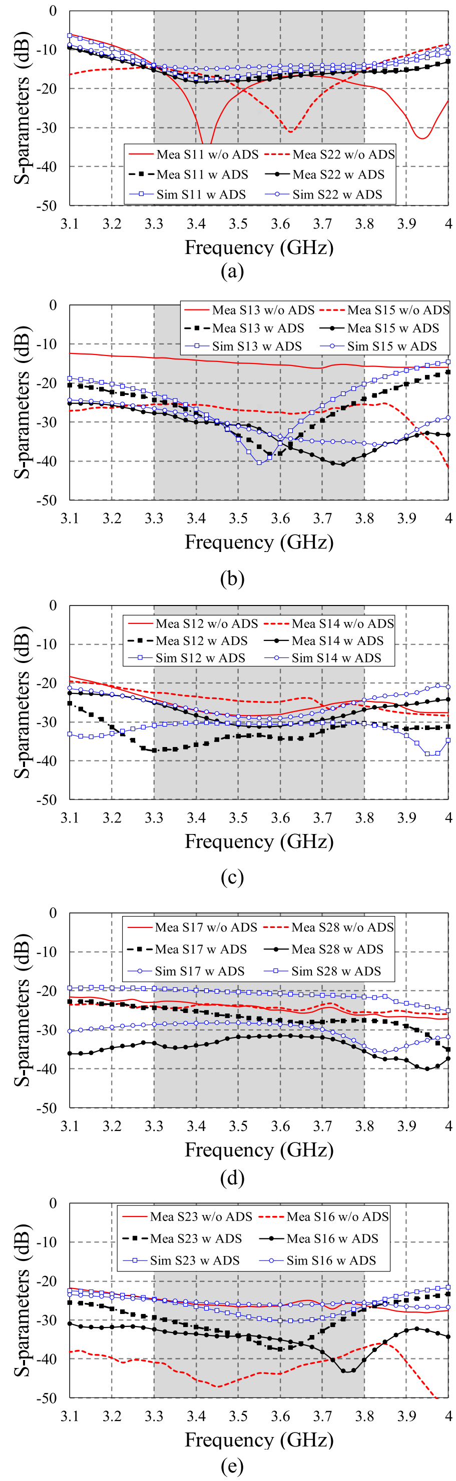

Fig. 14. Measured and EM simulated S-parameters of the 2 by 2 array with and without ADS. (a) S_{11} and S_{22}. (b) S_{13} and S_{15}. (c) S_{12} and S_{14}. (d) S_{17} and S_{28}. (e) S_{23} and S_{16}.

The mutual coupling between elements 1 and 6 is the weakest among others due to cross-polarization and a long separation distance. As shown in Fig. 14(e), with the ADS the coupling is changed from −40 to −30 dB, which is far below other mutual coupling and should not be a concern. In Fig. 14, the EM-simulated S-parameters for the array with the ADS are also provided, showing a conservative estimation.

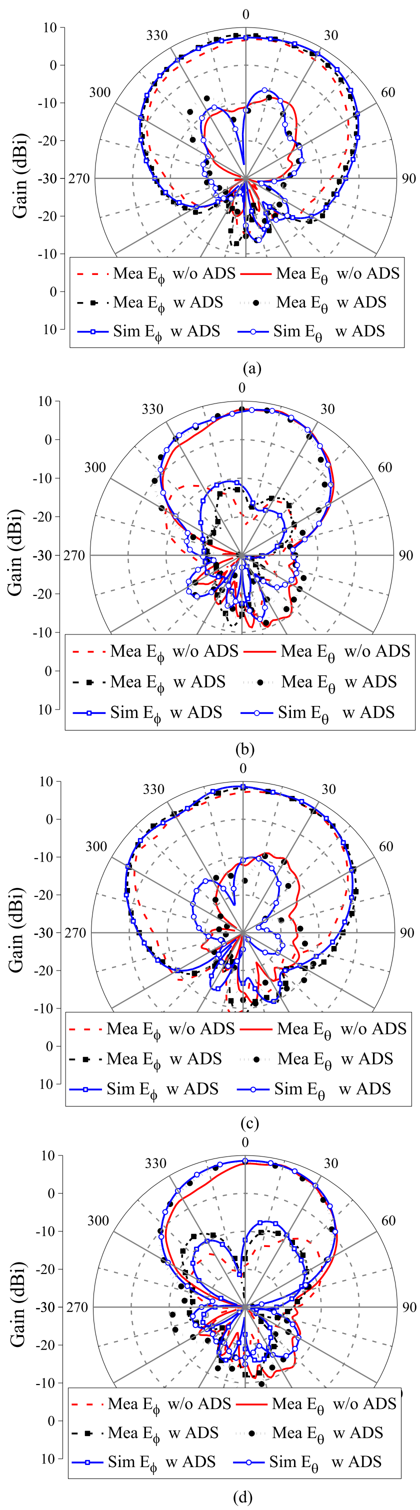

Fig. 15. Representative radiation patters of the 2 by 2 dual-polarized dipole array with and without the ADS. (a) H-plane patterns of element 1. (b) E-plane patterns of element 1. (c) H-plane patterns of element 2. (d) E-plane patterns of element 2.

One of the attractive attributes of the ADS method is its radiation pattern enhancement capability. It is known that due to the existence of mutual coupling the active radiation pattern of each antenna element in an array will be distorted. This issue can be alleviated after an ADS is applied. Fig. 15 shows the radiation patters of antenna elements 1 and 2 with and without the ADS measured at 3.5 GHz in both H- and E-planes. By inspecting the radiation patterns, the following observations can be obtained.

1) The beam widths of the major field components for an antenna element with the ADS are about the same as those of the element without the ADS, but are with less distortion due to the reduction of mutual coupling.
2) Antenna gain is enhanced.
3) The ratio of forward/backward radiation for an element with and without the ADS is about the same.
4) A good cross-polarization ratio can be retained, i.e., better than 18 and 10 dB in axial and in ±60° directions, respectively.

The measured (Mea) active radiation patters of antenna elements with the ADS are also verified by EM simulation (Sim) at 3.5 GHz, as superimposed in Fig. 15. Excellent correlation can be observed.

V. Conclusion

A new concept called ADS for reducing mutual coupling between both co- and cross-polarized antenna elements in a large-scale array antenna is proposed. An ADS is a thin surface that primarily consists of a plurality of metal reflection patches and is placed above the array antenna. The partially reflected waves from the ADS can be controlled to create interference signal to the coupled waves among adjacent antenna elements, leading to a high degree of cancellation of the unwanted mutual coupling in a wide frequency band. Design guidelines and considerations of the ADS are discussed. Two practical design examples are given in detail and the usefulness of the ADS is demonstrated by applying commonly used precoding schemes to array antennas. The attractive features of the ADS include the applicability to a large-scale array antenna; the suitability for a wide range of antenna forms; a wide decoupling bandwidth; and, above all, the simplicity in implementation. It is expected that the ADS can be widely used in communication and radar applications, where the phased array technology is used.

References

[1] H. Q. Ngo, E. G. Larsson, and T. L. Marzetta, “Energy and spectral efficiency of very large multiuser MIMO systems,” *IEEE Trans. Commun.*, vol. 61, no. 4, pp. 1436–1449, Apr. 2013.

[2] T. L. Marzetta, “Noncooperative cellular wireless with unlimited numbers of base station antennas,” *IEEE Trans. Wireless Commun.*, vol. 9, no. 11, pp. 3590–3600, Nov. 2010.

[3] J. L. Allen and B. L. Diamond, “Mutual coupling in array antennas,” Dept. Lincoln Lab., Massachusetts Inst. Technol., Lexington, MA, USA, Tech. Rep. 424 (ESD-TR-66-443), 1966.

[4] Q. Yuan, Q. Chen, and K. Sawaya, “Performance of adaptive array antenna with arbitrary geometry in the presence of mutual coupling,” *IEEE Trans. Antennas Propag.*, vol. 54, no. 7, pp. 1991–1996, Jul. 2006.

[5] B. Wang, Y. Chang, and Y. Sun, “Performance of the large-scale adaptive array antennas in the presence of mutual coupling,” *IEEE Trans. Antennas Propag.*, vol. 64, no. 6, pp. 2236–2245, Jun. 2016.

[6] R. Janaswamy, “Effect of element mutual coupling on the capacity of fixed length linear arrays,” *IEEE Antennas Wireless Propag. Lett.*, vol. 1, no. 1, pp. 157–160, 2002.

[7] J. W. Wallace and M. A. Jensen, “Mutual coupling in MIMO wireless systems: A rigorous network theory analysis,” *IEEE Trans. Wireless Commun.*, vol. 3, no. 4, pp. 1317–1325, Jul. 2004.

[8] C. Masouros, M. Sellathurai, and T. Ratnarajah, “Large-scale MIMO transmitters in fixed physical spaces: The effect of transmit correlation and mutual coupling,” *IEEE Trans. Commun.*, vol. 61, no. 7, pp. 2794–2804, Jul. 2013.
[9] K.-H. Chen and J.-F. Kiang, “Effect of mutual coupling on the channel capacity of MIMO systems,” *IEEE Trans. Veh. Technol.*, vol. 65, no. 1, pp. 398–403, Jan. 2016.
[10] D. M. Pozar, “A relation between the active input impedance and the active element pattern of a phased array,” *IEEE Trans. Antennas Propag.*, vol. 51, no. 9, pp. 2486–2489, Sep. 2003.
[11] L. Savy and M. Lesturgie, “Coupling effects in MIMO phased array,” in *Proc. IEEE Radar Conf. (RadarConf)*, Philadelphia, PA, USA, May 2016, pp. 1–6.
[12] J. Andersen and H. Rasmussen, “Decoupling and descattering networks for antennas,” *IEEE Trans. Antennas Propag.*, vol. 24, no. 6, pp. 841–846, Nov. 1976.
[13] L. Zhao, L. K. Yeung, and K.-L. Wu, “A coupled resonator decoupling network for two-element compact antenna arrays in mobile terminals,” *IEEE Trans. Antennas Propag.*, vol. 62, no. 5, pp. 2767–2776, May 2014.
[14] K. Qian, L. Zhao, and K.-L. Wu, “An LTCC coupled resonator decoupling network for two antennas,” *IEEE Trans. Microw. Theory Techn.*, vol. 63, no. 10, pp. 3199–3207, Oct. 2015.
[15] L. D. Bamford, J. R. James, and A. F. Fray, “Minimising mutual coupling in thick substrate microstrip antenna arrays,” *Electron. Lett.*, vol. 33, no. 8, pp. 648–650, Apr. 1997.
[16] F. Yang and Y. Rahmat-Samii, “Microstrip antennas integrated with electromagnetic band-gap (EBG) structures: A low mutual coupling design for array applications,” *IEEE Trans. Antennas Propag.*, vol. 51, no. 10, pp. 2936–2946, Oct. 2003.
[17] L. Zhao and K.-L. Wu, “A decoupling technique for four-element symmetric arrays with reactively loaded dummy elements,” *IEEE Trans. Antennas Propag.*, vol. 62, no. 8, pp. 4416–4421, Aug. 2014.
[18] F. Rusek *et al.*, “Scaling up MIMO: Opportunities and challenges with very large arrays,” *IEEE Signal Process. Mag.*, vol. 30, no. 1, pp. 40–60, Jan. 2013.
[19] C. B. Peel, B. M. Hochwald, and A. L. Swindlehurst, “A vector-perturbation technique for near-capacity multiantenna multiuser communication—Part I: Channel inversion and regularization,” *IEEE Trans. Commun.*, vol. 53, no. 1, pp. 195–202, Jan. 2005.
[20] Y. Gou, S. Yang, J. Li, and Z. Nie, “A compact dual-polarized printed dipole antenna with high isolation for wideband base station applications,” *IEEE Trans. Antennas Propag.*, vol. 62, no. 8, pp. 4392–4395, Aug. 2014.

Ke-Li Wu (M’90–SM’96–F’11) received the B.S. and M.Eng. degrees from the Nanjing University of Science and Technology, Nanjing, China, in 1982 and 1985, respectively, and the Ph.D. degree from Laval University, Quebec, QC, Canada, in 1989.

From 1989 to 1993, he was with the Communications Research Laboratory, McMaster University, Hamilton, ON, Canada, as a Research Engineer and the Group Manager. In 1993, he joined the Corporate Research and Development Division, COM DEV International, Cambridge, Ontario, Canada, the largest Canadian space equipment manufacturer, where he was a Principal Member of Technical Staff. Since 1999, he has been with The Chinese University of Hong Kong, Hong Kong, where he is currently a Professor and the founding Director of the Radiofrequency Radiation Research Laboratory. He has authored or co-authored numerous publications in the areas of electromagnic (EM) modeling and microwave passive components, microwave filter, and antenna engineering. His current research interests include partial element equivalent circuit and derived physically expressive circuit EM modeling of high-speed circuits, RF and microwave passive circuits and systems, synthesis theory and practices of microwave filters, antennas for wireless terminals, decoupling techniques for array antennas, and RF identification technologies.

Prof. Wu was a recipient of the 1998 COM DEV Achievement Award in 2008 and the Asia-Pacific Microwave Conference Prize in 2012. He is a Member of the IEEE MTT-8 Subcommittee (Filters and Passive Components) and also serves as a TPC Member for many prestigious international conferences including the International Microwave Symposium. From 2006 to 2009, he was an Associate Editor of the IEEE Transactions on MTT.

Changning Wei received the B.S. degree in electronic engineering from the University of Science and Technology of China, Hefei, China, in 2014. He is currently pursuing the Ph.D. degree with The Chinese University of Hong Kong, Hong Kong.

His current research interests include antenna design, antenna decoupling techniques, and large-scale massive multiple-input multiple-output antenna array for advanced wireless communications.

Xide Mei received the B.S. degree in electronic engineering from the University of Electronic Science and Technology of China, Chengdu, China, in 2015. He is currently pursuing the Ph.D. degree with The Chinese University of Hong Kong, Hong Kong.

His current research interests include antenna design, wireless channel modeling, and design of multiple-input multiple-output antenna array by incorporating wireless channel models.

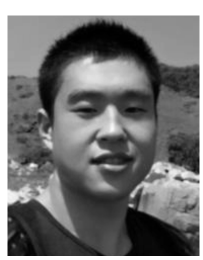

Zhen-Yuan Zhang received the B.S. degree in electronic science and engineering from the Nanjing University of Posts and Communications, Nanjing, China, in 2011, and the M.S. degree in electronic engineering from The Chinese University of Hong Kong, Hong Kong, in 2013, where he is currently pursuing the Ph.D. degree in eletronic engineering.

His current research interests include circularly polarized antenna design, wideband base station antenna design, and antenna decoupling techniques.